Machine Learning Assisted Multi-Objective Planar Antenna Array Synthesis for Interference Mitigation in Next Generation Wireless Systems

Sahiti Vankayalapati* and **Lakshman Pappula**

Abstract—The exponential increase of data traffic in next generation wireless communication attracts optimized design of antenna arrays (AAs) to be deployed in RANs. The traditional antenna array synthesis techniques have become exhaustive leading to the introduction of machine learning assisted new binary optimization algorithm. In this paper, three specific AA features are given particular attention: peak sidelobe level (PSLL), first null beam width (FNBW), and broad sector null in interference directions. These contrast each other, and a multi-objective new binary cat swarm optimization (MO-NBCSO) with a novel mutation probability is developed to derive the best-compromised solutions among them. The computational complexity is approximated as $O(MN^2)$ (here, M and N represent the number of objectives and population size, respectively). Hence, a 20×20 planar antenna array is considered for synthesis and pare to fronts are generated alongside state-of-the-art MO algorithms. A fuzzy-based decision approach is introduced to choose the best trade-off solutions. A detailed comparative performance study is carried out by the two-performance metrics, namely, I-metric and S-metric. Numerical results illustrate that MO-NBCSO is a better candidate to produce the best antenna arrays in terms of array characteristics over other algorithms.

1. INTRODUCTION

High gain antennas arrays with beamforming, null forming capability are instrumental in 5G/6G deployment scenarios for the RANs to meet the new demands of the end users. The wireless data traffic has expanded significantly in the past five years due to huge upload and download of data for different use cases and newly evolving applications. Requirements of the end users continue to increase exponentially, setting high demands on RANs to provide greater coverage, better throughput and higher capacity. The peak data rates of 6G are shifting towards terabits per second (Tbps). Thus, we require large antenna arrays [1] (AAs) with advanced beamforming techniques at the base stations in RANs. Large AAs are wide apertured and formed by large number of antenna elements. The synthesis of these arrays is mechanically complex and is not cost effective. So aperiodic array synthesis can be realized by altering the positions of the array elements using thinning technique. A thinned antenna array is one that has a reduced number of array elements in comparison with an array that is equally spaced and has multiple advantages [2]. Despite its superiority, finding the best possible combinational switch ON and OFF states of elements in large AAs to induce aperiodicity is cumbersome.

The increased use of radio energy in the data transmission and reception process has polluted the free space radiation environment to a more significant extent. So, to avoid unwanted interference null synthesis with significant null depth should be performed. Though they are dependent, the reduction of the SLL and the null depth are individually significant in the synthesis process. Also, tactical thinning

suppresses the peak sidelobe level (PSLL), but it significantly affects the shape of the principal lobe called first null beam width (FNBW). AAs should be capable of producing radiation patterns with low PSLL while maintaining a narrow FNBW, null placement in interfering directions to increase the efficiency of communication thereby enhancing the data rates. A significant increase in the performance of the above parameters cannot be observed without sacrificing the other. So, developing an objective function that will force the synthesis process to find feasible solutions by satisfying all the above concerns is essential. To meet all the goals, many researchers have proposed multi-objective (MO) optimization through machine learning [3–8] assisted algorithms as single objective algorithms fail to address the above. MO approaches offer the designer various possible solutions on the pareto-optimal front. One can arrive at the optimal solution by trading off a set of optimal solutions derived from the conflicting objectives. Dominance and Pareto-optimality are two fundamental parameters that drive the multi-objective solutions towards optima.

A binary MO optimization algorithm with exhaustive search needs to be developed, to explore the feasible solutions among a large pool of solutions and perform thinned array synthesis. Thinning is devised as a binary variable optimization technique where the solutions are encoded into binary strings. The swarm-based intelligence algorithms have been a breakthrough in recent years for various engineering applications. These are modeled by observing the natural behavior of different species. Among these, the real-valued cat swarm optimization (CSO) [9, 10] is popular and has shown its potential in solving various engineering problems [11–14]. It is formulated by mimicking the natural demeanor of the cat. The successful adoption of real-valued CSO in current research fueled the development of a new MO new binary version of CSO (MO-NBCSO). A few works in literature indicate the synthesis of a MO thinned linear array [11, 14, 15] but not planar antenna array (PAA). Most papers focus on single-objective thinned PAA synthesis problems in the literature. A little work has been carried out in multi-objective synthesis as of now. The major contributions in this work.

(i) The new binary version of MO-CSO, named MO-NBCSO is developed and applied to synthesize thinned PAA to control the shape of the radiation pattern.

(ii) A new mutation probability with a gaussian mutated tangent function is introduced in MO-NBCSO.

(iii) MO thinned PAA synthesis has been carried out in all ϕ planes.

(iv) Sector null in all ϕ planes has been introduced as one of the objectives.

(v) A fuzzy decision-making strategy has been introduced to AA synthesis to choose the best-compromised solution.

(vi) Performance metrics have been used to estimate the quality of the pareto optimal solutions produced by MO-NBCSO and competing binary optimization techniques.

2. MULTI-OBJECTIVE NEW BINARY CAT SWARM OPTIMIZATION (MO-NBCSO)

NBCSO is a novel algorithm that mimics a continuous version of CSO. The significant difference being the position vector is constructed using binary digits instead of real values. The main objective of NBCSO is to explain the notion of the adaptive nature of the cat to trace its prey and link its behavior to binary nature. To make our algorithm capable of solving multi-objective problems, the concept of non-dominated sorting [16] principle is used and named MO-NBCSO. Here the cat operates in two modes the seeking and tracing modes.

A mathematical model is formulated to represent both modes in NBCSO as follows. Let us consider a D-dimensional solution space, and the position of ith cat is represented by $X_{i,d} = (X_{i1}, X_{i2}, \ldots, X_{iD})$, and velocity by $V_{i,d} = (V_{i1}, V_{i2}, \ldots, V_{iD})$, here $d = 1$ to D which indicates the dimension. Evaluate the fitness of each cat for all the M objectives and rank the cats based on non-dominance [16]. An external archive is used to store the non-dominated solutions. Rank-based pareto fronts will be produced based on non-dominance. The cats are distributed into modes depending on the value specified by the mixture ratio (MR).

2.1. Seeking Mode (SM)

The cats always stay resting but are alert in observing the surrounding environment. If the cat makes a move for the next position, then it makes a prolonged move while observing the surroundings. The formulation of this nature and a few essential parameters of SM are discussed below.

 i Seeking memory Pool (SMP): It indicates the count of cat copies to be produced.

 ii Counts of dimension to change (CDC): The count of mutating dimensions.

 iii Mutation Probability (MP): The probability of occurrence of binary mutation is indicated by MP. CDC is taken as a reference to mutate the selected dimensions corresponding to the value specified by MP. This parameter is introduced in NBCSO to replace the seeking range of selected dimension parameter from the traditional CSO operating on a real coding.

 The steps involved in SM are given below:

1) Create k copies of the ith cat; here, SMP $= k$.

2) The mutation process is applied on $(k-1)$ copies of the ith cat among the available k copies. Based on the value of CDC and MP, each dimension (binary value) of the ith cat is to be mutated. The mutation probability of the parent cat in each dimension is represented by $MP(X_{i,d}^k)$.

$$MP\left(X_{i,d}^k\right) = 1 + \frac{1}{2}\tanh\left(\frac{-D_{i,d}^k - Z}{2}\right) + \frac{1}{2}\tanh\left(\frac{D_{i,d}^k - Z}{2}\right) \tag{1}$$

where $k = 1,\ldots,k-1$ and $d = 1,\ldots,D$. $X_{i,d}^k$ represents the position of kth copy of the ith cat in the dth dimension. The symbol $D_{i,d}^k$ indicates the spread distance generated by the standard gaussian number, and the mutation control parameter (Z) is a constant. The gaussian mutation number initializes the slight movement of the cat in positive and negative directions. This move authorizes more minor mutations in the parent's neighborhood. It leads to a more organized search around the cat position and makes the search capabilities of NBCSO more promising. The mutation probability has the range $[0,1]$ by limiting the sigmoid transformation maps. The mutation bit is represented by the equation below, which is obtained after calculating the rn value in the range of $[0,1]$.

The ith cat is updated using the below equation.

$$Y_{i,d}^k = \begin{cases} 1, & if \quad \left(rn < MP\left(X_{i,d}^k\right)\right) \\ 0, & else \end{cases} \tag{2}$$

$$X_{i,d}^{k+1} = \text{mod}\left(x_{i,d}^k + y_{i,d}^k, 2\right). \tag{3}$$

The cat's natural behavior is mathematically modeled, and the justification and flow of the mechanism are depicted below. In SM, the cat displacement is significantly less as it observes the environment around it. The mathematical equation should create a scope where the position updation is much less. It can be done when the mutation rate is less. To facilitate this, the mathematical equation is modeled as in Equation (1). The rate of mutation is directly related to the mutation probability. The gaussian mutation number with the proper value of Z in the tangent function allows lower mutation probability values over larger values. The mutation probability for the various values of Z is depicted in Fig. 1. The value of $Z = 6$ yields the best-synthesized arrays, and the respective numerical illustrations are discussed in Section 6. The mutation happens if at least one bit in the string is updated. The displacement of the cat will be large if two or more bits among the string are updated. Thus, Equations (1), (2), and (3) are modeled to allow the cat to explore the search space more systematically around the original position by limiting larger displacements. Equations (2) and (3) are formulated to derive the characteristics of the cat into binary strings from the value of MP.

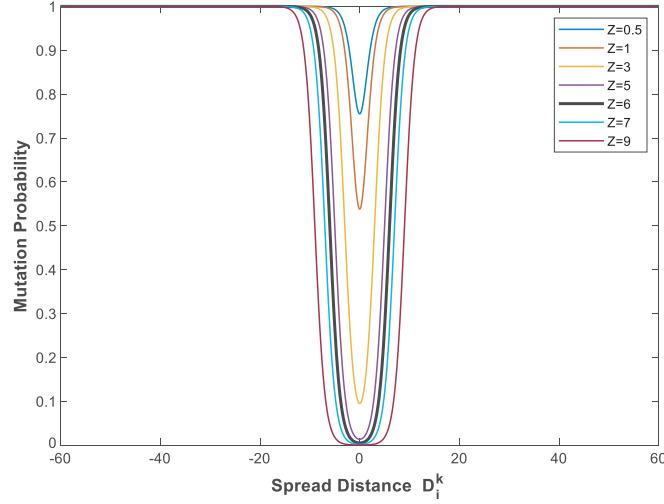3) Evaluate the cats' fitness value for all the M objectives.

Figure 1. MP versus spread distance around the cat position for the various values of Z.

2.2. Tracing Mode (TM)

TM is another sub-model where the cats are not resting but trace the targets by spending a lot of energy. The change in the position of the cat is mathematically modeled in this mode and the process remains the same as in [17].

After completing the SM and TM evolutionary processes, the updated combined SM and TM cats undergo the non-dominating sorting along with the cats in the external archive. The MO-NBCSO evolutionary process is continued until the maximum iteration count is reached. The pseudo-code of MO-NBCSO is summarized in algorithm 1 from lines 1 to 24.

2.3. Fuzzy Decision Making

When a pareto front produces many solutions at its center, it becomes cumbersome to derive solutions that give equal weight age to each considered objective; providing a solution with high precision is difficult for any decision-making technique. There is a certain amount of fuzziness in every objective. In such a scenario, fuzzy decision-making can use to arrive at a compromised solution [18]. The amount of fuzziness is derived from the membership functions. The membership function of the ith function of the jth objective for a pareto optimal front is given by the below equation.

$$\mu_i^j = \begin{cases} 1 & if \quad f_i \leq f_i^{\min} \\ \dfrac{f_i^{\max} - f_i}{f_i^{\max} - f_i^{\min}} & if \quad f_i^{\min} < f_i \leq f_i^{\max} \\ 0 & if \quad > f_i^{\min} \end{cases} \tag{4}$$

μ_i^j indicates the efficiency with which the jth nondominated solution can satisfy the objective function. When N nondominated solutions are present, the below equation gives the efficiency of achieving each non-dominated solution.

$$\mu_i^j = \frac{\displaystyle\sum_{i=1}^{M} \mu_i^j}{\displaystyle\sum_{j=1}^{N}\sum_{i=1}^{M} \mu_i^j} \tag{5}$$

Here M is the total number of objectives, and the decision maker can accept a compromised solution with the μ_i^j value with maximum.

Algorithm 1 Multi-objective New Binary Cat Swarm Optimization (MO-NBCSO)

1: **procedure**
2:     Set all parameters M, NP, SMP, SRD, CDC, and *Maximum Iterations*.
      Initialize apopulation of cats and the velocity for each cat(solution)
3:     Evaluate the fitness of each cat
4:     $A = \varphi$ ▷ A is an archive to store all non-dominated solutions
5:     Update A ▷ Extract non-dominated solutions from the initial
                     population and store in A
6:     **while** (Termination condition is not met) **do**
7:       Separate the population of cats for seeking mode and tracing mode based on MR
8:       **for** $i = 1 \leftarrow S_s$, **do** ▷ S_s is the number of cats in the seeking mode
9:         **for** $j = 1 \leftarrow SMP - 1$ **do**
10:           Select the CDC number of dimensions to vary
11:           Based on SRD, mutate the ith using Equations (1) to (3)
12:           Check the variables' range
13:           Compute fitness for each mutated solution
14:         **end for**
15:       **end for**
16:       **for** $k = 1 \leftarrow S_t$ **do** ▷ S_t is the number of cats in the tracing mode
17:         Find the new position of the jth cat using Equations in TM[17]
18:         Check the variables' range
19:         Compute the fitness of the new cat position
20:       **end for**
21:       Update archive A with the new cat positions
22:     **end while**
23:     **return** the archive A
24: **end procedure**

2.4. Computational Complexity of MO-NBCSO

The computational complexity is approximated based on the evolutionary process of MO-NBCSO as outlined in algorithm 1 and a few assumptions are made. As in practice, the least case of the loops is considered because it significantly affects the estimation of computational time. The effect of the size of D on computational complexity is ignored as it is a small number compared to the size of N and A. Also, the lines having constant complexities are ignored.

The computational complexity for line 3 is $O(MN)$ as it computes the fitness values of all the population for M objectives. Line 4 has constant computational complexity $O(1)$ as it initializes A with a null set. The non-dominated sorting for the solutions of initialized cats is computed in line 5, and the corresponding complexity is represented as $O(MN^2)$ [16]. In line 7, S_s and S_t number of cats will participate in SM and TM evolutionary process based on MR, and the respective computational complexity is represented as $O(N)$. The SM process is depicted in lines 8 to 15. In this process, a total of S_s (SMP-1) cats will undergo a mutation process according to CDC and Equations (1) to (3). The fitness of these mutated cats for M objectives will be calculated. The corresponding computational complexity of lines 8 to 15 is represented as $O(MS_s$ (SMP-1)). In lines 16 to 20, the computational complexity for the updated S_t cats and computing their fitness values for M objectives in the TM process is represented as $O(MS_t)$. The population, including the parent cats and updated mutated cats, is sorted in line 21, and the resulting computational complexity is $O(MN^2)$. The maximum input value of the MO-NBCSO evolutionary process is observed as N. Hence, considering all the steps involved in MO-NBCSO, the least case of computational complexity is approximated as $O(MN^2)$. It is

the same as the computational complexity of NSGA-II [16] and MO-BCSO [2] with the non-dominating sorting mechanism.

3. CHARACTERISTICS OF A PLANAR ARRAY

The planar array [17], which is symmetric about the x-axis and y-axis, is constructed by a geometry of $2Q \times 2R$ elements.

$$AF(\mathbf{I},\, \theta\varphi) = 4 \sum_{r=1}^{R} \sum_{q=1}^{Q} I_{rq} \cdot \cos\left[\pi \cdot (r - 0.5) \cdot U\right] \cos\left[\pi \cdot (q - 0.5) \cdot V\right] \tag{6}$$

where $U = \sin(\theta)\cos(\phi)$, $V = \sin(\theta)\sin(\phi)$, $\phi(0 \leq \phi \leq \pi)$ is the angle in the elevation plane, and I_{rq} represents the amplitude excitation of the (rq) elements witch ON (with 1) and OFF (with 0). The elements of the planar array as placed at 0.5λ from each other.

4. PROBLEM FORMULATION FOR MULTI-OBJECTIVE SYNTHESIS

The effect of minimization of PSLL in planar antenna array synthesis has been observed and discussed below after a detailed survey of work in the literature. The general 3-Dimensional radiation pattern of a uniformly illuminated 20×20 planar array in Fig. 2 shows that high sidelobe levels exist in principle planes ($\phi = 0°$ & $90°$). Quite often, researchers exercise their algorithms on reducing the SLLs only in the principal planes to project the effectiveness of the proposed algorithm. But, if the PSLL in $\phi = 0°$ and $90°$ planes is reduced, then proportionately, the SLLs in other planes gradually increase. It does not abide by the proper flow of the synthesis mechanism. Instead, PSLL should be controlled in all ϕ planes. Only then is the algorithm said to be effective in finding the optimal values for the PAA synthesis. The objective functions in this section have been designed with the aim to synthesize a PAA having a radiation pattern with minimum PSLL and null sector in the desired range with narrow FNBW. These objectives contradict each other; therefore, a multi-objective trade-off mechanism is utilized to draw the best trade-off solutions.
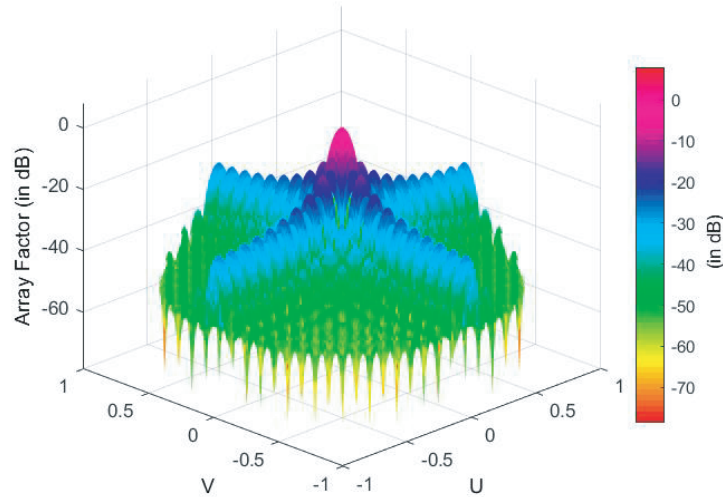

Figure 2. 3-Dimensional radiation pattern of uniformly illuminated 20×20 planar antenna array.

4.1. Realization of Objective 1

The first fitness function is formulated to minimize the peak sidelobe level in the entire ϕ-plane.

$$f_1 = \left(\left| \frac{AF(\theta, \phi)}{AF(\theta, \phi)_{\max}} \right| \right) \Bigg|_{\theta \in \text{ sidelobe region on the entire } \phi\text{-plane}} \tag{7}$$

Here $AF(\theta, \phi)_{\max}$ is the maximum value of the main beam, and f_1 is limited to the region between θ and ϕ excluding the main beam. In other words, f_1 is limited to the sidelobe region.

4.2. Realization of Objective 2

The objective function is formulated to obtain a sector null in a predefined angular region in the entire ϕ-plane.

$$f_2 = \left(\sum_{i=j}^{k} AF(\theta_i) \right) \Bigg|_{For\ all\ \phi\ \text{planes}} \tag{8}$$

here j and k indicate the start and end limits of the azimuth angle for the null sector in the sidelobe region.

4.3. Realization of Objective 3

The original array's FNBW characteristic must be maintained during the synthesis process in the entire ϕ-plane. The fitness function to achieve this is formulated as

$$f_3 = \max \left(\theta_{fni} : \ i = 1, 2, \dots \phi_i \right) \tag{9}$$

where θ_{fni} is the position of the first null in the ith plane.

5. THINNED PLANAR ANTENNA ARRAY SYNTHESIS USING MO-NBCSO

In this section, a large thinned PAA having size 20×20 (400 elements) is synthesized. MO-NBCSO along with traditional MO binary genetic algorithm (MO-BGA) [19], MO particle swarm optimization (MO-BPSO) [20], and MO binary cat swarm optimization (MO-BCSO) [21] are used to produce the best possible pareto-optimal solutions between the objectives. Algorithms have been used to perform thinning by finding suitable combinations of 1's and 0's. Two test cases have been considered for

Table 1. Parameter composition of MO-NBCSO, MO-BCSO, MO-PSO, and MO-BGA.

Algorithm	Parameter with value
MO-NBCSO	SMP = 3; CDC = 80%; MR = 0.8; $Z = 6$ Inertia weight (ω): a linear decrease from 0.9 to 0.2 Acceleration coefficient (C) = 2; Random number (r) = generated between 0 and 1
MO-BCSO	SMP = 3; CDC = 20%; MR = 0.8; PMO = 0.2 ωr same as NBCSO
MO-BPSO (archive-based non-dominance)	Size of the archive = 100; C = $2\,\omega$ a linear decrease from 0.9 to 0.4
MO-BGA (non-dominating)	Simulated binary cross-over distribution index = 20; Pool size = 50; Tour size = 2 Polynomial mutation distribution index = 20

simulation to demonstrate the performance of the proposed method. The initial parameter setup for all the algorithms is given in Table 1. Sensitivity analysis has been carried out to select the best parametric values of MO-NBCSO to suit this application. All the algorithms are executed for 50 runs. The quality of the best-compromised pareto optimal solution has been measured with two performance metrics, S [22] and I [23, 24]. In general, the MO optimization is twofold: To drive the algorithm towards finding the solutions that are as close to the pareto front as possible; To find the solutions having the maximum diversity on the nondominated front. The significance of the first objective is to guide the solutions toward the pareto optimal region. Once a significant pareto optimal front is achieved, the second goal aids in identifying the best solutions having great diversity on the pareto front. The best values are marked in bold in the tables. All the simulations have been carried out using MATLAB on windows operating laptop with processor i3-8100T CPU at 3.10 GHz, and 4 GB RAM. The number of function evaluations is considered as 20,000. The mean performances in terms of performance metrics have been recorded.

5.1. Case 1: Trade-Off between PSLL, FNBW and Null Depth at $\theta = (25° \, to \, 29°)$ in All ϕ Planes ($\phi = 0° \, to \, 90°$)

In this case, MO-NBCSO and other algorithms are applied to generate the best pareto-optimal solutions by trading off PSLL, FNBW and null depth at $\theta = (25° \, to \, 29°)$ with sector width of $5°$ in the entire ϕ-plane. The best pareto fronts produced in one of the 50 runs by MO-NBCSO, MO-BCSO, MO-BPSO, and MO-BGA are shown in Fig. 3(a). The fuzzy logic-based decision maker defined by Equations (4) and (5) is used to choose the best compromised pareto-optimal solution among the solutions obtained by each of the algorithms and the same is shown in Fig. 3(b). The respective MO-NBCSO optimized AA input configuration (ON and OFF status) is given in Table 3. The thinning percentage of the antenna
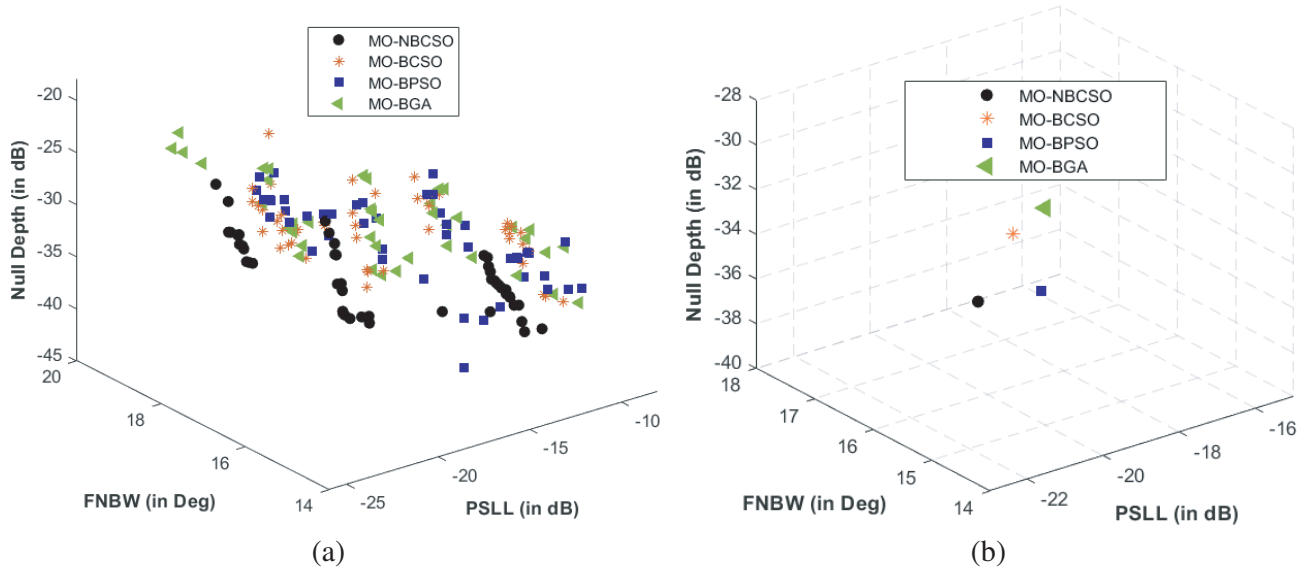

Figure 3. (a) Pareto fronts obtained by a trade-off between PSLL, FNBW, and Null depth. (b) Best trade-off solution set visualization attained using fuzzy decision maker.

Table 2. Compromised solutions obtained based on fuzzy logic.

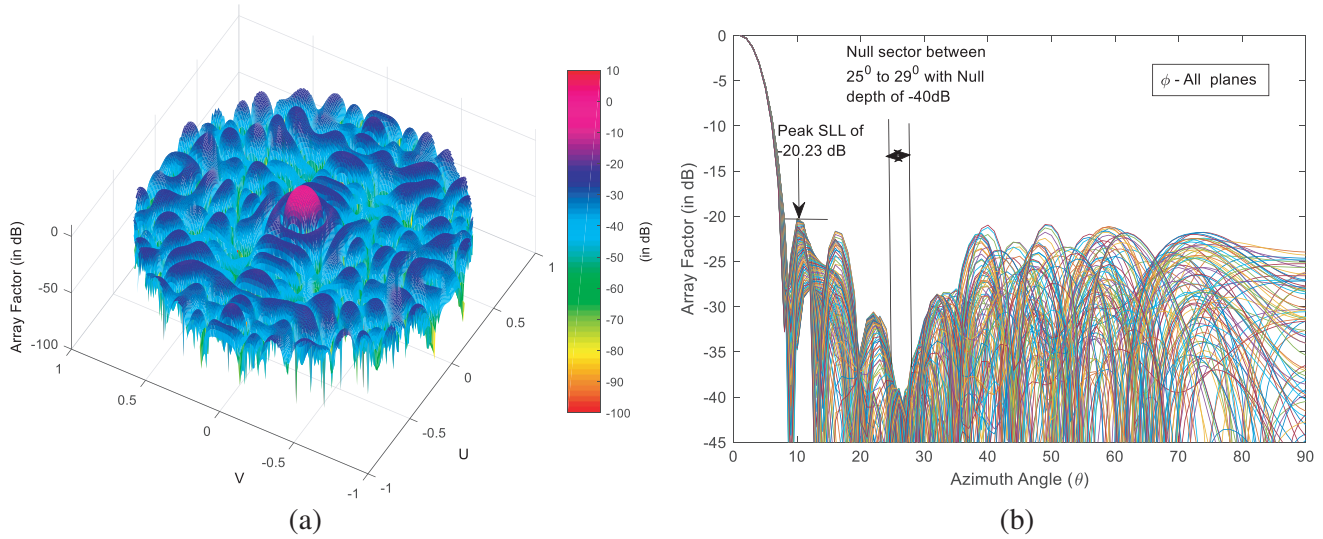| Objectives	MO-NBCSO	MO-BCSO	MO-BPSO	MO-BGA
$\mathbf{f_1}$ PSLL (in dB)	-20.23	-19.24	-18.57	-18.47
$\mathbf{f_2}$ Null depth (in dB)	-38.13	-33.16	-36.14	-32.47
$\mathbf{f_3}$ FNBW (in deg)	$16°$	$16°$	$16°$	$18^{0°}$

Figure 4. (a) The 3-Dimensional radiation pattern. (b) 2-Dimensional radiation pattern in all planes with a null depth of -40 dB in the angular region of $25°$ to $29°$.

Table 3. Elements ON and OFF status for MO-NBCSO arrays for Case I and Case II.

Case I	Case II
1 1 1 1 0 1 1 1 1 0	1 1 1 1 1 1 1 1 1 0
1 1 1 0 1 1 1 1 0 1	1 1 1 1 1 0 1 1 0 0
1 1 1 1 1 1 1 0 1 1	1 1 1 1 1 0 1 0 1 1
0 1 1 0 1 1 1 1 0 1	1 1 1 1 1 1 1 1 1 1
1 1 1 0 1 0 1 0 1 0	1 1 1 1 1 1 0 0 1 0
1 1 1 0 1 0 0 1 0 1	1 0 1 1 0 0 1 1 1 0
0 1 1 1 1 1 1 0 0 0	1 1 0 0 1 0 0 0 1 0
1 1 1 1 0 0 0 0 1 0	1 0 1 1 0 1 1 0 0 0
1 1 0 0 1 0 0 0 0 0	1 1 1 0 1 0 0 0 0 0
1 0 1 1 0 1 0 1 0 0	0 1 0 1 0 1 0 0 0 0

elements using MO-NBCSO is 37% which indicates 148 elements were switched OFF out of 400 total array elements. The thinning rate for MO-BCSO is 37%; MO-BPSO is 38%; and MO-BGA is 42%.

The radiation characteristics for the best-compromised solutions obtained by all algorithms are given in Table 2. Even the suppression of small amounts of PSLL in the entire ϕ-plane is considered a good achievement during comparison among algorithms. Figs. 4(a), 4(b) show the 3-Dimensional, 2-Dimensional far-filed radiation patterns of the MO-NBCSO respectively. The 2-Dimension far-filed radiation pattern is provided from $\theta = 0°$ to $90°$ due to symmetry of planar structure along the X and Y direction gives better visualization of null depth and FNBW. MO-NBCSO produced PSLL of -20.23 dB with a sector null of depth -38.13 dB in the angular sector region of $\theta = 25°$ to $29°$ in the entire ϕ-plane whichis evident from Fig. 4(b). MO-NBCSO has 1 dB, 1.66 dB, and 1.76 dB lower PSLL compared to MO-BCSO, MO-BPSO, and MO-BGA. All the algorithms produce similar FNBW except MO-BGA. The null sector is formed in the whole radiation pattern-like ring with a sector width of $5°$ as seen in Fig. 4(a). Sector null depths were observed as -37.73 dB, -33.16 dB, -36.14 dB, and -32.47 dB for MO-NBCSO, MO-BCSO, MO-BPSO, and MO-BGA algorithms, respectively.

Tables 4 and 5 depict the qualitative S and I performance metrics for all the chosen algorithms. MO-NBCSO produces lower values of S-metric, compared to the other three algorithms. A low value

Table 4. Statistical results for S-metrics for case-I.

	Performance metric	MO-NBCSO	MO-BCSO	MO-BPSO	MO-BGA
S	Best	**0.9065**	1.5232	0.9933	1.0704
	Worst	**1.0137**	1.7489	1.2194	1.4528
	Mean	**0.9463**	1.6012	1.1059	1.3172
	Standard Deviation	**0.0355**	0.0809	0.0939	0.1218

Table 5. Statistical results for I-metrics for case-I.

	Performance metric	MO-NBCSO	MO-BCSO	MO-BPSO	MO-BGA
I	Best	**1690.43**	1494.54	1431.27	1354.21
	Worst	**1510.33**	902.12	846.76	842.32
	Mean	**1616.63**	1185.52	1075.45	1022.72
	Standard Deviation	**64.12**	165.75	176.02	131.77

indicates a uniform spread of solutions in the pareto front. MO-NBCSO produced high values compared to other three algorithms for I-metric analysis, which portrays MO-NBCSO ability to exhibit higher diversity among optimal solutions on the pareto front. The mean value obtained with MO-NBCSO is more than the values produced with other algorithms. MO-NBCSO has a significantly smaller standard deviation and indicates stability in achieving a similar solution in every run for both the metrics. MO-NBCSO yields better S and I metric values over MO-BCSO, MO-BPSO, and MO-BGA.

5.1.1. Sensitivity Analysis

The sensitivity analysis is carried out to demonstrate the selection of the appropriate value of Z. Simulations have been carried out on different Z values as specified in Fig. 1. At the same time, all other parameters of MO-NBCSO are kept constant, as mentioned in Table 1. The I-metric values were observed as 1264.41, 1444.32, 1588.57, 1616.63, 1375.45, and 1386.24 for the Z values 1, 3, 5, 6, 7, and 9, respectively. The simulated values of the S-metric for the Z same values were observed as 1.11, 1.21, 1.19, 1.01, 1.03, and 1.15. It's decided that the best choice of the Z value for the MO-NBCSO algorithm is 6. The sensitivity analysis is performed for other parameters and the best tuned values are as mentioned in Table 1 are selected for the synthesis process. It is clear from all the tables and figures that MO-NBCSO showed better performance over other algorithms. Hence, MO-NBCSO is a better candidate for multi-objective synthesis problems.

5.2. Case II: Trade-off between PSLL, FNBW, and Null Depth at $\theta = (32° \, to \, 35°)$ in selective ϕ planes (at $\phi = 35°$, $36°$, $37°$)

In this case, a null sector in a few desired planes ($\phi = 35°$ to $37°$) has been considered for synthesis along with suppression of PSLL in all ϕ planes and maintaining narrow FNBW. To achieve this the objective function 2 is reformulated as

$$f_2 = \left(\sum_{i=j}^{k} AF(\theta_i) \right) \Bigg|_{For \ \phi=35^0 \, to \, 37^0 \text{ planes}} \tag{10}$$

All the algorithms have been applied to obtain the best possible pareto fronts. The best pareto fronts obtained by MO-NBCSO and competing algorithms among the 50 runs are shown in Fig. 5(a). The best compromised pareto optimal solutions using the fuzzy logic-based decision maker from each of the simulated algorithms are shown in Fig. 5(b). The respective antenna performance metrics of each of the
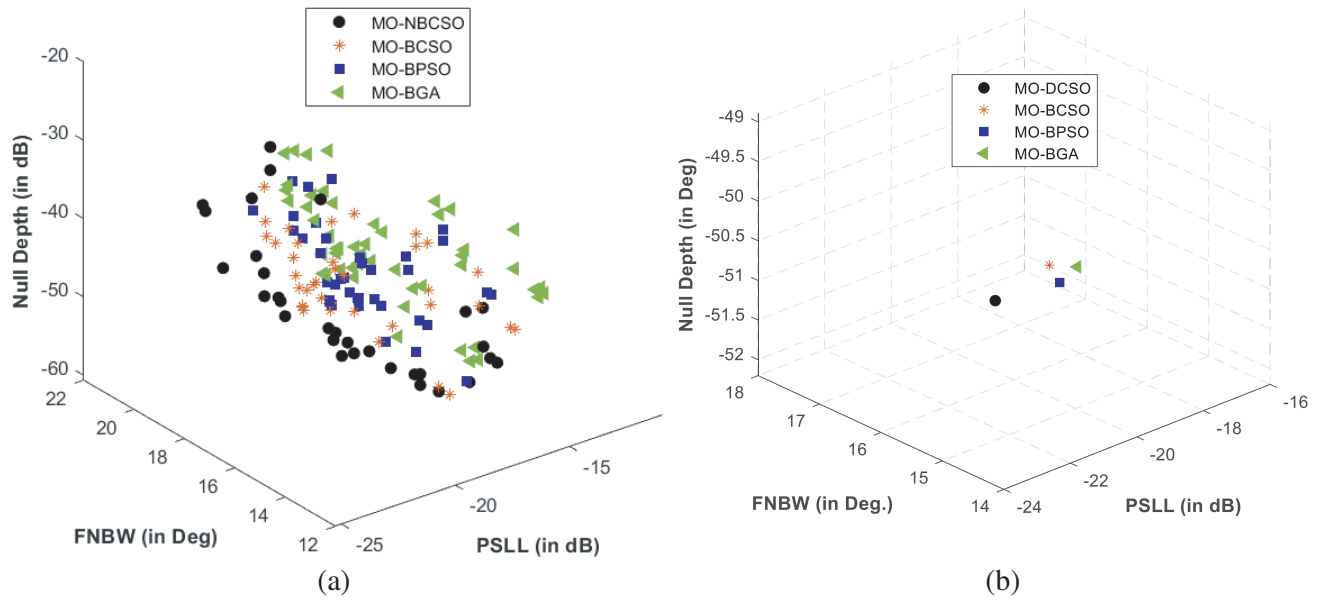
Figure 5. (a) Pareto optimal obtained for case II. (b) The best trade-off solution set visualization attained using fuzzy decision maker.

Table 6. Compromised solutions obtained based on fuzzy logic in case of desired planes of ($\phi = 35°$, $36°$, $37°$).

Objectives	MO-NBCSO	MO-BCSO	MO-BPSO	MO-BGA
$\mathbf{f_1}$ PSLL (in dB)	-20.5666	-18.9396	-18.6302	-18.1022
$\mathbf{f_2}$-Null depth (in dB)	-52.1051	-50.9271	-51.197	-51.0869
$\mathbf{f_3}$ FNBW (in deg)	$16°$	$16°$	$16°$	16^0

compromised solutions are listed in Table 6. MO-NBCSO produced PSLL of -20.56 dB, whereas MO-BCSO, MO-BPSO, and MO-BGA produced -18.9396 dB, -18.6302 dB, and -18.1022 dB, respectively. MO-NBCSO achieved 1.63 dB, 1.93 dB, and 2.46 dB low PSLL compared to MO-BCSO. MO-NBCSO achieved a significant reduction in PSLL compared to other algorithms. As discussed in case 1, it is worth mentioning that obtaining a low PSLL value in all the ϕ planes that satisfy other criteria is a complex task for the algorithms.

The array structure (ON and OFF status) for the MO-NBCSO solution with 37% thinning is provided in Table 3. The percentage of thinning for MO-BCSO was 37%, MO-BPSO was 36%, and MO-BGA was 35%. The 3-D dimension radiation pattern concerning this array structure is shown in Fig. 6(a). Fig. 6(b) represents the 2-Dimensional plot of far filed radiation pattern to analyze the depth of the sector nulls at $\theta = (32°$ to $35°)$ on ($\phi = 35°$ to $37°$) planes. Deep sector nulls with a null depth of -52.10 dB can be observed clearly, as highlighted in Figs. 6(a) and (b). It has been observed that -52.10 dB of the maximum null level has been obtained by MO-NBCSO in the null sector angular range while maintaining low PSLL and narrow FNBW. All the algorithms exhibit a narrow FNBW of $16°$. Hence, it can be observed from a detailed discussion that MO-NBCSO outperforms the other three algorithms in achieving low PSLL and deep null depths with maintaining narrow FNBW.

Deep null depths in the given null sector angular region were observed in case 2 over case 1 due to the selection of ϕ planes. All ϕ planes were considered in case1, whereas selected planes were considered in case 2 for null placements. MO-NBCSO and the other three algorithms were assessed using the S and I-performance metrics to comment on the quality of the obtained solutions. The statistical process of S
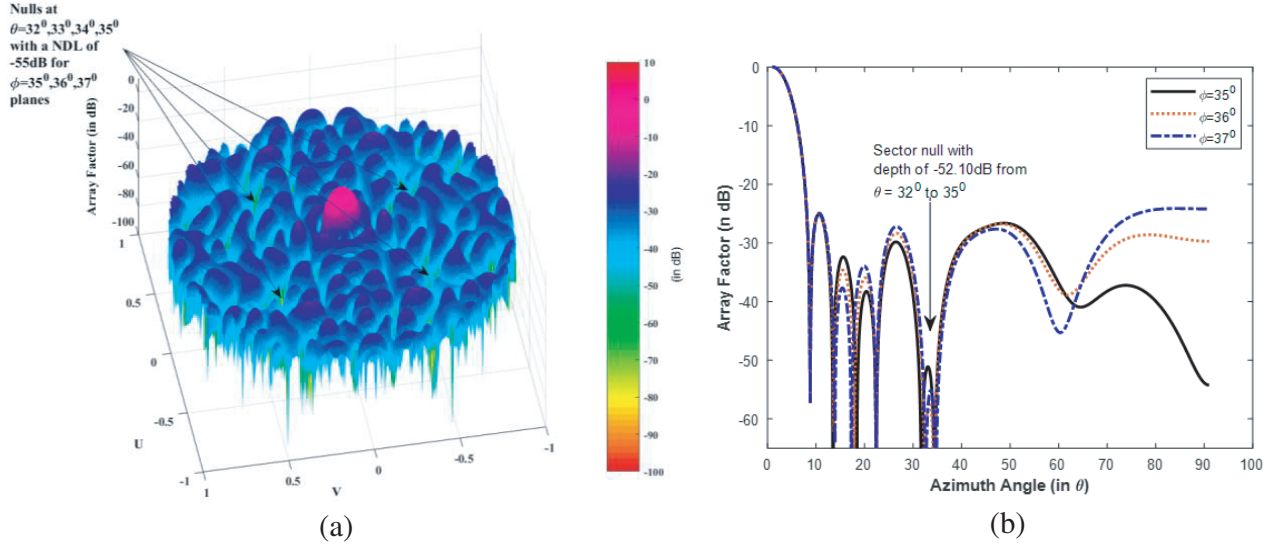
(a)   (b)

Figure 6. (a) 3-Dimensional radiation pattern. (b) 2-Dimensional far-field obtained by MO-NBCSO compromised antenna array in selective ϕ (at 35°, 36°, 37°) plane.

Table 7. Statistical results for S-metrics for case-II.

Performance metric		MO-NBCSO	MO-BCSO	MO-BPSO	MO-BGA
S	Best	**0.8977**	1.5222	0.7999	1.3265
	Worst	**0.9947**	1.7389	1.9993	1.8755
	Mean	**0.9334**	1.6144	1.7227	1.5892
	Standard Deviation	**0.0301**	0.0753	0.3327	0.1921

Table 8. Statistical results for I-metrics for case-II.

Performance metric		MO-NBCSO	MO-BCSO	MO-BPSO	MO-BGA
I	Best	**2172.4**	2028.5	2040.3	1749.2
	Worst	**1989.3**	1754.4	1658.4	1528.6
	Mean	**2056.2**	1850.9	1841.1	1634.6
	Standard Deviation	**74.8**	96.1	146.1	80.1

and I metrics for all the algorithms are provided in Tables 7 and 8, respectively. MO-NBCSO produced a high mean value of I-metric compared to the other three algorithms and exhibited high diversity of pareto-optimal solutions. MO-NBCSO delivers a low standard deviation value and exhibits more stability compared to the three different algorithms. It can be seen from Table 7 that the mean value of S-metric for MO-NBCSO is 0.9947, whereas the mean value obtained for MO-BCSO, MO-BPSO, and MO-BGA are 1.73, 1.99, and 1.87, respectively. A low value of S-metric for MO-NBCSO indicates that it produces a uniform spread of solutions on the pareto front.

6. CONCLUSION

A new machine learning assisted multi-objective binary optimization technique called MO-NBCSO has been developed for performing thinned PAA synthesis. A new mutation probability with a gaussian mutated tangent function is introduced in the algorithm to allow cat to explore the search space more systematically thereby improves the optimization procedure. A sensitivity analysis on important parameters of algorithm is carried out to select suitable parametric values. The performance of MO-NBCSO is compared with MO-BCSO, MO-BPSO, and MO-BGA to demonstrate the effectiveness of the proposed algorithm. A fuzzy-based decision-making strategy has been utilized to select the best compromised solutions. Also, I and S performance metrics were used to weigh the quality of the pareto-optimal solutions over the pareto front. A precise analysis of the performance metrics is done to assess the quality of acquired solutions. MO-NBCSO exhibited better diversity and uniform spread of pareto optimal solutions over the pareto front. It offers greater flexibility over other algorithms by producing optimal synthesized arrays. Experimental results indicate that the algorithm has produced good pareto optimal solutions by trading off PSLL, narrow FNBW, and deep sector null in a large 20×20 PAA in selected ϕ planes and entire ϕ-plane. The synthesized Large PAAs installed at the base stations can greatly enhance the performance of radio access networks due to sector null placement incorporated in the design of the AA. This will aid in better management of jammers and other interfering devices which increases the overall performance of 6G communication.

REFERENCES

1. Lv, Y., F. Cao, X. Feng, and H. Li, "Improved binary particle swarm optimization and its application to beamforming of planar antenna arrays," *Progress In Electromagnetics Research C*, Vol. 114, 217–231, 2021.

2. Pappula, L. and D. Ghosh, "Aynthesis of thinned planar antenna array using multiobjective normal mutated binary cat swarm optimization," *Applied Computational Intelligence and Soft Computing*, Vol. 2016, Article ID 4102156, 2016.

3. Chen, W., Q. Wu, C. Yu, H. Wang, and W. Hong, "Multibranch machine learning-assisted optimization and its application to antenna design," *IEEE Trans. Antennas Propag.*, Vol. 70, No. 7, 4985–4996, 2022.

4. Akinsolu, M. O., K. K. Mistry, B. Liu, P. I. Lazaridis, and P. Excell, "Machine learning-assisted antenna design optimization: A review and the state-of-the-art," *2020 14th European Conference on Antennas and Propagation (EuCAP)*, Copenhagen, Denmark, 2020.

5. Lecci, M., P. Testolina, M. Rebato, A. Testolin, and M. Zorzi, "Machine learning-aided design of thinned antenna arrays for optimized network level performance," *14th Eur. Conf. Antennas Propagation, EuCAP 2020*, 2020.

6. El Misilmani, H. M., T. Naous, and S. K. Al Khatib, "A review on the design and optimization of antennas using machine learning algorithms and techniques," *Int. J. RF Microw. Comput. Eng.*, Vol. 30, No. 10, 2020.

7. Baumgartner, P., T. Bauernfeind, O. Biró, et al., "Multi-objective optimization of Yagi-Uda antenna applying enhanced firefly algorithm with adaptive cost function," *IEEE Trans. Magn.*, Vol. 54, No. 3, 2018.

8. Koziel, S. and A. Bekasiewicz, "Pareto-ranking bisection algorithm for expedited multiobjective optimization of antenna structures," *IEEE Antennas Wirel. Propag. Lett.*, Vol. 16, 1488–1491, 2017.

9. Ram, G., D. Mandal, R. Kar, and S. P. Ghoshal, "Cat swarm optimization as applied to time-modulated concentric circular antenna array: Analysis and comparison with other stochastic optimization methods," *IEEE Trans. Antennas Propag.*, Vol. 63, No. 9, 4180–4183, 2015.

10. Ahmed, A. M., T. A. Rashid, and S. A. M. Saeed, 'Cat swarm optimization algorithm: A survey and performance evaluation," *Comput. Intell. Neurosci.*, Vol. 2020, 2020.

11. Bhargav, A. and N. Gupta, "Multiobjective genetic optimization of nonuniform linear array with low sidelobes and beamwidth," *IEEE Antennas Wirel. Propag. Lett.*, Vol. 12, 1547–1549, 2013.

12. Pappula, L. and D. Ghosh, "Linear antenna array synthesis using cat swarm optimization," *AEU — Int. J. Electron. Commun.*, Vol. 68, No. 6, 540–549, 2014.

13. Bianchi, D., S. Genovesi, and A. Monorchio, "Constrained pareto optimization of wide band and steerable concentric ring arrays," *IEEE Trans. Antennas Propag.*, Vol. 60, No. 7, 3195–3204, 2012.

14. Pal, S., "Optimal synthesis of linear antenna arrays with multi-objective differential evolution," *Progress In Electromagnetics Research B*, Vol. 21, 87–111, 2010.

15. Pappula, L. and D. Ghosh, "Aynthesis of aperiodic linear antenna array using multi-objective cat swarm optimization," *2015 Int. Conf. Microwave, Opt. Commun. Eng. ICMOCE 2015*, 231–234, 2016.

16. Deb, K., A. Pratap, S. Agarwal, and T. Meyarivan, "A fast and elitist multiobjective genetic algorithm: NSGA-II," *IEEE Trans. Evol. Comput.*, Vol. 6, No. 2, 182–197, 2002.

17. Vankayalapati, S., L. Pappula, and D. Ghosh, "Element thinning using discrete cat swarm optimization for 5G/6G applications," *Progress In Electromagnetics Research B*, Vol. 101, 119–135, 2023.

18. Pradhan, P. M. and G. Panda, "Pareto optimization of cognitive radio parameters using multiobjective evolutionary algorithms and fuzzy decision making," *Swarm Evol. Comput.*, Vol. 7, 7–20, 2012.

19. Nebro, A. J., E. Alba, G. Molina, F. Chicano, F. Luna, and J. J. Durillo, "Optimal antenna placement using a new multi-objective CHC algorithm," *Proc. GECCO 2007 Genet. Evol. Comput. Conf.*, 876–883, 2007.

20. Jin, N. and Y. Rahmat-Samii, "Advances in particle swarm optimization for antenna designs: Real-number, binary, single-objective and multiobjective implementations," *IEEE Trans. Antennas Propag.*, Vol. 55, No. 3, 556–567, 2007.

21. Sharafi, Y., M. A. Khanesar, and M. Teshnehlab, "Discrete binary cat swarm optimization algorithm," *2013 3rd IEEE Int. Conf. Comput. Control Commun. IC4 2013*, 1–6, 2013.

22. Schott, J. R., "Fault tolerant design using single and multicriteria genetic algorithm optimization," Massachusetts Institute of Technology, 1995.

23. Eckart, Z. and T. Lothar, "SPEA: Multiobjective evolutionary algorithms: A comparative case study," *IEEE Trans. Evol. Comput.*, Vol. 3, No. 4, 257–271, 1999.

24. Pradhan, P. M. and G. Panda, "Connectivity constrained wireless sensor deployment using multiobjective evolutionary algorithms and fuzzy decision making," *Ad Hoc Networks*, Vol. 10, No. 6, 1134–1145, 2012.